Article

Immunity

Toll-like Receptor 4 Engagement on Dendritic Cells Restrains Phago-Lysosome Fusion and Promotes Cross-Presentation of Antigens

Graphical Abstract

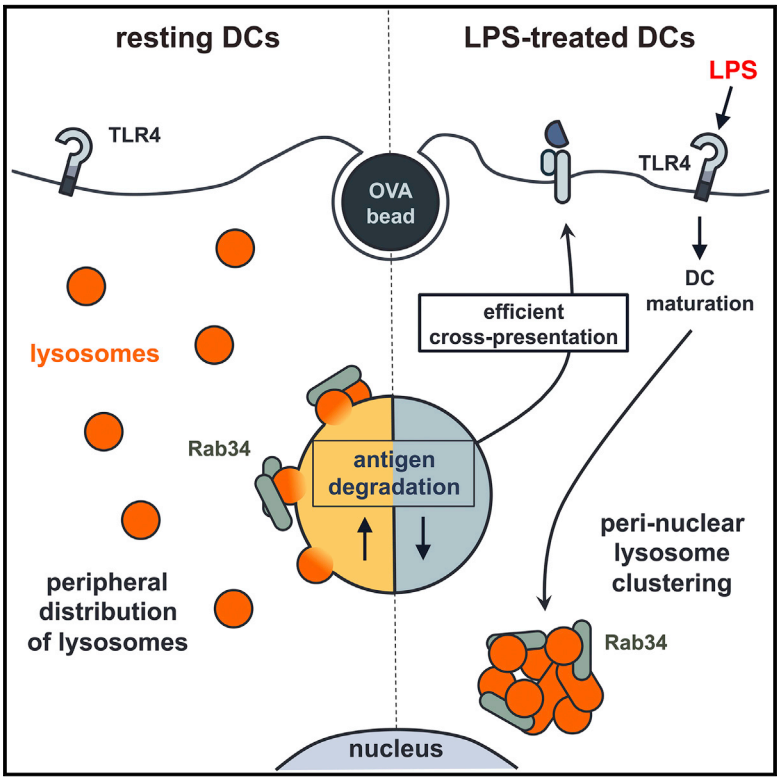

Authors

Andrés Alloatti, Fiorella Kotsias, Anne-Marie Pauwels, ..., Rudi Beyaert, Eik Hoffmann, Sebastian Amigorena

Correspondence

eik.hoffmann@irc.vib-ugent.be (E.H.), sebastian.amigorena@curie.fr (S.A.)

In Brief

During DC maturation, cross-presentation is first upregulated and then turned off. Amigorena and colleagues show now that during a transient phase after TLR4 engagement, which lasts up to 18 hr, DC maturation results in the topological re-organization of lysosomes by Rab34. This decreases phago-lysosome fusion and strongly enhances cross-presentation efficiency.

Highlights

- TLR4 engagement of DCs for 16 hr increases cross-presentation in vivo and in vitro
- Phagosomes of maturing DCs recruit less lysosomal enzymes becoming less degradative
- LPS-treated DCs display clustering of lysosomes and reduced phago-lysosomal fusion
- Rab34 controls lysosome organization thus increasing cross-presentation efficiency

Alloatti et al., 2015, Immunity *43*, 1087–1100
December 15, 2015
http://dx.doi.org/10.1016/j.immuni.2015.11.006

CellPress

Immunity
Article

Toll-like Receptor 4 Engagement on Dendritic Cells Restrains Phago-Lysosome Fusion and Promotes Cross-Presentation of Antigens

Andrés Alloatti,[1,10] Fiorella Kotsias,[1,2,10] Anne-Marie Pauwels,[3,4] Jean-Marie Carpier,[1] Mabel Jouve,[5] Evy Timmerman,[6,7] Luigia Pace,[1] Pablo Vargas,[1,8] Mathieu Maurin,[1] Ulf Gehrmann,[1] Leonel Joannas,[1] Omar I. Vivar,[1] Ana-Maria Lennon-Duménil,[1] Ariel Savina,[1,9] Kris Gevaert,[6,7] Rudi Beyaert,[3,4,11] Eik Hoffmann,[1,3,4,11,*] and Sebastian Amigorena[1,11,*]

[1]INSERM U932, Institute Curie, 75248 Paris Cedex 05, France
[2]Department of Virology, Faculty of Veterinary Sciences, University of Buenos Aires, 1427 Buenos Aires, Argentina
[3]Inflammation Research Center, Unit of Molecular Signal Transduction in Inflammation, VIB, 9052 Ghent, Belgium
[4]Department of Biomedical Molecular Biology, Ghent University, 9000 Ghent, Belgium
[5]UMR3215, Institute Curie, 75248 Paris Cedex 05, France
[6]Department of Medical Protein Research, VIB, 9000 Ghent, Belgium
[7]Department of Biochemistry, Ghent University, 9000 Ghent, Belgium
[8]CNRS UMR 144, Institute Curie, 75248 Paris Cedex 05, France
[9]Roche SAS, 92650 Boulogne-Billancourt Cedex, France
[10]Co-first author
[11]Co-senior author
*Correspondence: eik.hoffmann@irc.vib-ugent.be (E.H.), sebastian.amigorena@curie.fr (S.A.)
http://dx.doi.org/10.1016/j.immuni.2015.11.006

SUMMARY

The initiation of cytotoxic immune responses by dendritic cells (DCs) requires the presentation of antigenic peptides derived from phagocytosed microbes and infected or dead cells to CD8$^+$ T cells, a process called cross-presentation. Antigen cross-presentation by non-activated DCs, however, is not sufficient for the effective induction of immune responses. Additionally, DCs need to be activated through innate receptors, like Toll-like receptors (TLRs). During DC maturation, cross-presentation efficiency is first upregulated and then turned off. Here we show that during this transient phase of enhanced cross-presentation, phago-lysosome fusion was blocked by the topological re-organization of lysosomes into perinuclear clusters. LPS-induced lysosomal clustering, inhibition of phago-lysosome fusion and enhanced cross-presentation, all required expression of the GTPase Rab34. We conclude that TLR4 engagement induces a Rab34-dependent re-organization of lysosomal distribution that delays antigen degradation to transiently enhance cross-presentation, thereby optimizing the priming of CD8$^+$ T cell responses against pathogens.

INTRODUCTION

Phagocytosis represents a critical innate barrier against infection and serves the clearance of extracellular microbes, infected and non-infected cells. After uptake, phagosomes undergo sequential fusion and fission events, first with endosomal and then lysosomal compartments leading to degradation of the phagosome content, a process referred to as "phagosome maturation" (Flannagan et al., 2009). Phagosome maturation includes the acquisition of hydrolases, NADPH oxidases, and vacuolar ATPases (Kinchen and Ravichandran, 2008). Mature phago-lysosomes display effective anti-microbial capacity.

In contrast to macrophages or neutrophils, which use phagocytosis for microbe destruction, phagocytosis in dendritic cells (DCs) mainly serves antigen processing and presentation (Savina and Amigorena, 2007). Major histocompatibility complex (MHC) class I presentation is classically restricted to endogenous antigens. However, also exogenous antigens can be presented on MHC I molecules in a process called cross-presentation, which is required for the initiation of cytotoxic immune responses against bacteria, tumors, certain viruses, and for the maintenance of self tolerance (Joffre et al., 2012). DCs have developed a specialized phagocytic pathway, which allows optimal conditions for cross-presentation (Savina and Amigorena, 2007). These specializations include a mildly degradative phagosomal environment, export of antigen to the cytosol for proteasome-mediated degradation, and effective loading of the generated peptides in the endoplasmic reticulum (ER) or in phagosomes (Guermonprez et al., 2003). Indeed, slow maturation and acidification of phagosomes (Savina et al., 2006, 2009), as well as limited degradation (Gil-Torregrosa et al., 2004; Lennon-Duménil et al., 2002; Inaba et al., 2000) are critical for cross-presentation.

Another direct consequence of phagosome specialization is the discrimination of self from non-self phagosomal cargo through engagement of pattern-recognition receptors. Cargoes that engage Toll-like receptors (TLRs) accelerate phagosome maturation in the first few hours after uptake. This effect is phagosome autonomous, as TLR engagement in one phagosome

does not affect the maturation of other phagosomes containing cargoes that do not engage TLRs (Blander and Medzhitov, 2006). By controlling phagosome maturation, TLR engagement promotes antigen presentation on both MHC I and II molecules. The mechanisms underlying the effects of TLR engagement on antigen presentation are, however, incompletely understood. Recently, the Blander laboratory has shown that TLR engagement during uptake of phagosomal cargo induces SNAP23-dependent recruitment of MHC I molecules from endosomal recycling compartments, thereby promoting cross-presentation in the first few hours after uptake (Nair-Gupta et al., 2014).

TLR engagement also initiates a complex gene expression program that transforms immature DCs into full effectors of immunity. DC maturation includes profound changes in morphology, cytoskeleton organization, and protein expression, either at the cell surface or as secreted mediators (Pierre et al., 1997; Reis e Sousa, 2006; Stuart and Ezekowitz, 2005). DCs lose their phagocytic capacity as they mature in response to lipopolysaccharide (LPS) both in vitro (Sallusto and Lanzavecchia, 1994; West et al., 2004), and in vivo (Wilson et al., 2006). Recent studies, however, showed that endocytosis and phagocytosis are actually only slowed down, and are even unaffected when mediated through certain phagocytic receptors, such as Fcγ receptors (Platt et al., 2010). Mature DCs also acidify their endocytic compartments more efficiently than immature DCs (Sepulveda et al., 2009; Trombetta et al., 2003). The ability of DCs to cross-present antigens is transiently enhanced in the first 20 hr after TLR stimulation and then down-modulated after 24–40 hr (Gil-Torregrosa et al., 2004). This can be physiologically relevant to enable activated DCs to enter a ''surveillance'' state that allows internalization of additional antigen before inducing effective T cell priming.

Here, we analyze how enhanced cross-presentation induced by LPS is determined by changes in phagocytic functions during the intermediate phases of DC maturation. We show that LPS induced a strong and selective delay in the fusion activity between phagosomes and lysosomes. This delay prevented excessive degradation of internalized antigen and promoted cross-presentation. Delayed phago-lysosome fusion in LPS-treated cells required Rab34-mediated re-distribution of lysosomes into a dense perinuclear cluster, and slowed down displacements of phagosomes along microtubules. These results describe a mechanism of inhibition of phago-lysosome fusion that functionally links innate pathogen sensing in DCs and antigen cross-presentation.

RESULTS

Maturing DCs Capture and Cross-Present Antigen to T Cells More Efficiently Than Resting Cells In Vitro or In Vivo

We have shown previously that 24–40 hr after activation by LPS, the efficiency of cross-presentation of antigen-immunoglobulin G immune complexes (ICs) is downregulated in vitro (Gil-Torregrosa et al., 2004), as also reported by others using other forms of antigen both in vitro and in vivo (Wilson et al., 2006; Wagner and Cresswell, 2012; Samie and Cresswell, 2015). Nevertheless, before this reduction in cross-presentation, DCs go through a transient phase of increased efficiency of cross-presentation (Gil-Torregrosa et al., 2004). To further investigate the duration of this transient phase, which was initially tested after 5 hr of LPS, we examined later time points of 16 and 24 hr of LPS stimulation, when the expression of co-stimulatory molecules and MHC II molecules on the DC surface was already high (Figure S1A and B). The octapeptide SIINFEKL (OVA amino acids 257–264), which is recognized by both B3Z (a Kb-restricted, OVA-specific $CD8^+$ T cell hybridoma) and OT-I (TCR transgenic Kb OVA-specific $CD8^+$ T lymphocytes, Kurts et al., 1996) T cells and does not need processing or proteasomal degradation, was presented with equal efficiency by LPS-treated and resting bone-marrow-derived DCs (BMDCs) (Figure 1A and S1C right panel). In contrast, cross-presentation of both bead-bound OVA (bbOVA, Figure 1B) and soluble OVA (sOVA, Figure 1C), to either OT-I or B3Z T cells, was increased in cells treated with LPS for 16 hr, as compared to resting BMDCs. After 24 hr, as shown previously (Gil-Torregrosa et al., 2004; Wagner and Cresswell, 2012), the efficiency of cross-presentation was reduced, as compared to both untreated, and cells treated with LPS for 16 hr (Figure S1C). Therefore, LPS induces a prolonged (up to 16 hr) phase of enhanced cross-presentation in maturing DCs, before it is down-modulated after 24 hr of stimulation (Figure S1C).

To investigate whether this prolonged phase of increased cross-presentation is also observed during activation of DCs in vivo, we gave mice LPS intraperitoneally followed by intravenous injection of bbOVA (14 hr later), sOVA, or OVA-IC (15.5 hr later) (Figure 1D). 16 hr after LPS injection, total splenic $CD11c^+$ cells (for sOVA or OVA-ICs) or $CD8^+$ T cells having phagocytosed beads (for bbOVA) were sorted (Figure S1G) and co-cultured with OT-I T cells to measure antigen-specific T cell activation. Sixteen hr after injection of LPS, $CD11c^+$ splenic DCs expressed increased amounts of co-stimulatory molecules, as compared to cells from mice injected with PBS (Figure S1D). Of note, the percentage of phagocytic DCs was reduced in LPS-treated mice, but the relative number of cells having phagocytosed 1 or 2 beads was the same (Figure S1G). As shown in Figures 1E and 1J, splenic DCs from LPS-treated mice cross-presented bbOVA (Figures 1E and 1F), sOVA (Figures 1G and 1H) and OVA-IC (Figures 1I and 1J) to OT-I T cells more efficiently than untreated mice (as assessed by increased expression of CD25 and CD69 in OT-I T cells). We conclude that DCs activated in vivo during 16 hr by LPS cross-present antigen more effectively than resting DCs.

LPS Induces a TLR4-Dependent Decrease in Degradation of Phagosomal Antigen and Phago-Lysosomal Fusion

To explore the mechanism underlying this temporary increase in cross-presentation, we first tested whether it is due to augmented antigen uptake (a transient, but very short increase in macropinocytosis was described previously, West et al., 2004). BMDCs treated with LPS for 16 hr still internalized bbOVA, but at lower rates than resting BMDCs (Figures S1H and S1I). Therefore, increased cross-presentation in LPS-treated cells cannot be explained by higher antigen uptake. To test other forms of phagocytic cargo, we analyzed the uptake of OVA-expressing *E. coli* and of ultraviolet C-irradiated $H2^{bm1}$ transformed mouse embryonic fibroblasts (dead cell-OVA). Phagocytosis of

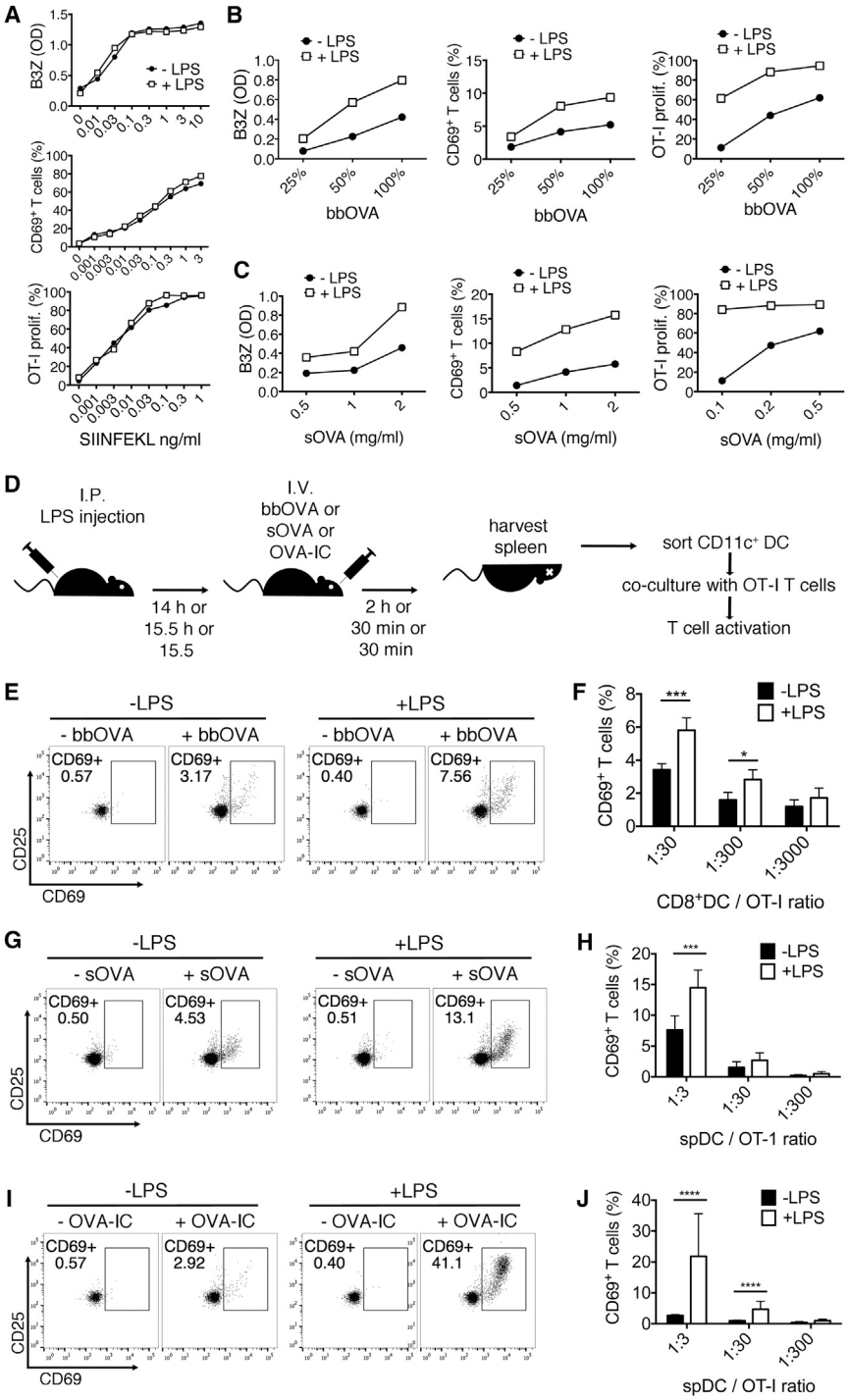

Figure 1. DC Matured In Vivo or In Vitro Are Able to Capture and Cross-Present Antigen More Efficiently Compared to Resting Cells

(A–C) BMDCs were incubated for 16 hr in presence (filled circles) or absence of 100 ng/ml LPS (open squares) before SIINFEKL peptide (A), bbOVA (B) and sOVA (C) were added. Cross-presentation efficiency of DCs was measured by co-culture with B3Z cells (left panel), CD69 expression of OT-I T cells (middle panel), and proliferation of CFSE-labeled OT-I T cells (right panel) (upper, middle, and lower panels, respectively, for Figure 1A). Shown is one representative out of three independent experiments.

(D) Experimental scheme for in vivo cross-presentation assays. OT-I T cell activation was measured by CD25 and CD69 expression, after co-culture for 16 hr with splenic DCs from mice non-treated (left panels) and systemically treated with LPS (right panels), immunized with bbOVA (E), sOVA (G), and OVA-IC (I).

(F, H, and J) Histograms display the average of three independent experiments for each of the mentioned antigens. Error bars represent SD. See also Figures S1 and S2.

E. coli, alive (Figure S2A), paraformaldehyde-fixed (Figure S2B), heat-killed (Figure S2C), and dead cell-OVA (Figure S2D) was observed in both resting and 16 hr LPS-activated BMDCs, always with lower efficiencies in LPS-treated cells.

We then investigated whether the transient increase in cross-presentation could be attributed to a temporary increase in antigen export to the cytosol using a previously described assay based on the enzymatic activity of β-lactamase (Cebrian et al., 2011). As shown in Figure S1J, after 16 hr of LPS treatment, antigen export to the cytosol was not significantly modified, as compared to resting BMDCs. Therefore, LPS-treated DCs cross-present phagosomal and endosomal antigens more efficiently than resting DCs, a difference that is not due to increased uptake or to changes in antigen export to the cytosol.

To further investigate how DC maturation favors cross-presentation, we characterized the degradative capacity of phagosomes and fusion with lysosomes in resting and 16 hr LPS-treated BMDCs, using bbOVA and single organelle-based flow cytometry (Savina et al., 2010). This technique allows simultaneous analysis of OVA degradation and acquisition of lysosomal markers (e.g., LAMP-1) exclusively in phagocytosed beads. In resting BMDCs, the proportion of beads bearing low amounts of OVA (due to degradation) and high amounts of LAMP-1 (due to phagosome maturation into phago-lysosomes) increased over time (Figure 2A). Similar results were found when lysosomes were pre-loaded with fluorescently labeled wheat germ agglutinin (WGA) before bead internalization (Figures S3A–S3D), indicating effective fusion between phagosomes and lysosomes. In 16 hr LPS-treated cells (100 ng/ml, Figure 2A or 10 ng/ml, Figures S3E and S3F), very few phagosomes with low OVA amounts and high LAMP-1 amounts appeared over time, indicating reduced degradation of OVA and delayed phagosome fusion with

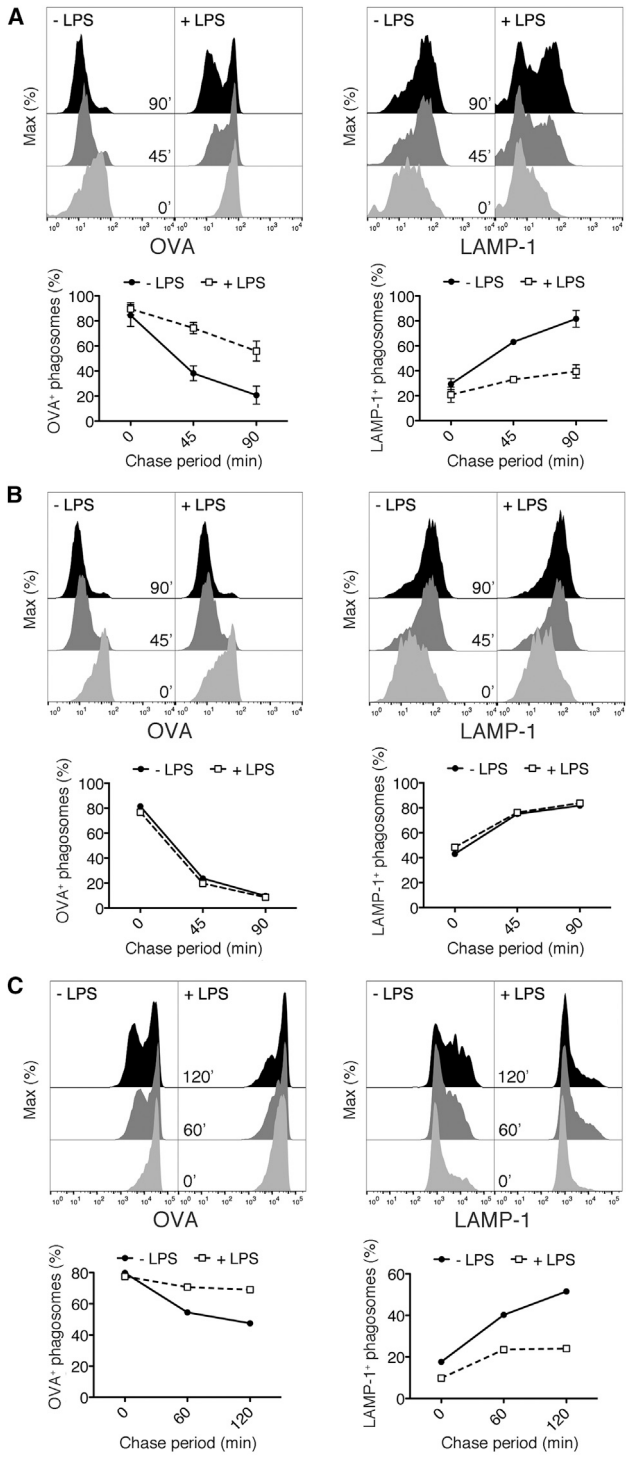

Figure 2. Activation of TLR4 by LPS Leads to Delayed Phagosomal Antigen Degradation

DCs were incubated for 16 hr in presence or absence of 100 ng/ml LPS before bbOVA was phagocytosed. Phagosome maturation was analyzed by flow organellocytometry in WT BMDCs (A), TLR4-deficient BMDCs (B), and splenic DCs (C). Histograms depict phagosomal OVA degradation (left panel) as well as phagosomal acquisition of LAMP-1 (right panel) after different chase periods. The data displayed here is a representative example of three independent experiments. See also Figures S1, S3, and S5.

lysosomes. Similarly, the proportion of WGA-positive phagosomes was very low in LPS-treated BMDCs, as compared to resting cells (Figure S3B). Reduced phago-lysosome fusion was also observed after 12 hr, but not after 6 hr, of LPS stimulation (Figures S3G and S3H). In addition, a similar reduction in phagosomal OVA and LAMP-1 proportions was observed after treating splenic DCs with LPS (Figure 2C and S1F). Reduced phago-lysosomal fusion was not observed when BMDCs lacked expression of TLR4 (Figure 2B), which as expected did not mature in response to LPS (Figure S1E). We conclude that 16 hr after engagement of TLR4, a substantial proportion (up to 50%) of phagosomes, in both BMDCs and splenic DCs, fail to effectively degrade OVA or to fuse with lysosomes.

Phagosomes of Resting DCs Are Highly Enriched in Lysosomal Enzymes

Reduced OVA degradation and increased acquisition of LAMP-1 or WGA in phagosomes suggest reduced fusion with lysosomes. In order to perform a more detailed analysis of the composition of phagosomes in resting and LPS-treated BMDCs, phagosomes were purified, and their proteome was analyzed using a quantitative shotgun approach that allows analysis of different samples simultaneously and offers evaluation of changes in protein composition in an unbiased and comprehensive manner. After lysis, phagosomal proteins were precipitated, digested, and labeled (Figure S4A). Phagosomal proteins of resting cells were labeled with light propionate ($^{12}C_3$), whereas proteins of LPS-treated cells were labeled with heavy propionate ($^{13}C_3$). Since equal amounts of both samples were mixed prior to liquid chromatography-tandem mass spectrometry (LC-MS/MS) analysis, the mass difference of labeled peptides further allowed a quantitative enrichment analysis (Figure S4B).

The identified phagosomal proteins found in two independent datasets were analyzed according to their functional categories. Proteins of lysosomal origin (V type proton ATPase, hydrolases), and proteins involved in vesicular trafficking and proteasomal degradation, as well as ER-associated proteins, are shown in Table 1. The majority of lysosomal hydrolases, including LAMP-1, LAMP-2, cathepsin B and D, and subunits of the V-type proton ATPase complex, were all enriched in phagosomes of resting BMDCs. Most proteins involved in fusion and vesicular trafficking, including syntaxins, Vps proteins, and Rab GTPases, as well as ER- and proteasome-related proteins, were found in similar proportions in resting and LPS-treated BMDC phagosomes.

We confirmed some of the LC-MS/MS results using Western blotting by comparing amounts of LAMP-1 and cathepsin D after loading equal amounts of protein (Figure S4C). Rab7 and gp91phox (a membrane subunit of the NADPH oxidase complex), were found in similar amounts in phagosomes from resting and activated BMDCs (Figure S4C). Phagosome lysates were devoid of Ykt6, a SNARE molecule involved in retrograde transport from Golgi to the ER that has been shown previously to be absent in purified DC phagosomes (Cebrian et al., 2011), confirming purity of the phagosome preparations in this study.

IRAP (an antigen-trimming peptidase), as well as the antigen peptide transporter TAP2, were found in phagosomes from both resting and LPS-treated BMDCs, whereas the MHC I molecule H-2K^b was clearly enriched in phagosomes from

LPS-treated DCs (Figure S4D). Other MHC I molecules, tapasin and, less notably, MHC II molecules, were also enriched in phagosomes from LPS-treated DCs, but the number of identified unique peptides was low. Altogether, these results show that phagosomes from resting BMDCs are enriched in proteins of lysosomal origin, as compared to phagosomes from LPS-treated DCs, indicating that LPS induces a reduction in fusion between phagosomes and lysosomes.

LPS Induces Perinuclear Clustering of Lysosomes in Maturing DCs

To better understand at the single cell level the observed reduction in phago-lysosome fusion, we used confocal immunofluorescence and cryo-immunoelectron microscopy. In resting BMDCs, LAMP-1 positive organelles showed a wide peripheral distribution (Figure 3A, upper panel). In contrast, the majority of LPS-treated BMDCs exhibited peri-nuclear clustering of LAMP-1-positive compartments and were devoid of these organelles in the cell periphery (Figure 3A, lower panel). The majority of phagocytosed bbOVA in resting cells was positive for LAMP-1 (Figure 3B, upper panel; Figures 3C and 3E), while most phagosomes in LPS-treated cells were not (Figure 3B, lower panel; Figures 3D and 3E). We observed a clear correlation in LPS-treated BMDCs between the peri-nuclear clustering of LAMP-1-positive compartments and phagosomes devoid of LAMP-1.

To investigate the mechanism involved, we next visualized fusion between fluorescent lysosomes and phagosomes using time-lapse video microscopy and LifeAct-GFP-expressing BMDC cultures. We analyzed the duration between uptake (formed phagosomes were positive for GFP-actin) until they acquired fluorescent WGA that was pre-loaded into lysosomes. All phagosomes in resting BMDCs rapidly acquired lysosomal WGA (Figure 4A and Movie S1), while BMDCs treated with LPS were heterogeneous in terms of phago-lysosome fusion. Certain cells displayed rapid fusion between lysosomes and phagosomes, which was comparable to resting cells. In others, fusion between phagosomes and lysosomes was hardly visible (Figure 4B). Those LPS-treated cells that showed reduced fusion also displayed peri-nuclear clustering of lysosomes (Figures 3A and 3B). To quantify these results, we first measured the time between phagosome formation (accumulation of fluorescent F-actin around the beads) and fusion with lysosomes (fluorescent WGA around the beads). In both resting and LPS-treated DCs, when it occurred, fusion with lysosomes took place on average 20 min after uptake (Figure 4C, black symbols). In LPS-treated BMDCs, however, we found an additional population of cells in which phagosomes did not fuse with lysosomes, even 180 min after uptake (Figure 4C, red symbols). This population of BMDCs almost exclusively displayed peri-nuclear clustering of lysosomes (Figure 4D). The results were quantified measuring the relative area covered by lysosomal compartments using a quantitative and automated Fiji macro. Values between 0.5 and 0.8 are characteristic of a wide peripheral distribution of lysosomes (a value of 1 means the total cell area is occupied by these organelles). In contrast, values between 0.1 and 0.4 correspond to lysosome clustering. LPS-treated BMDCs showed significantly lower values than resting BMDCs indicating lysosome clustering (Figure 4E). Therefore, as suggested by our previous observations, lysosomes are organized in tight perinuclear clusters only in LPS-treated BMDCs that fail to fuse phagosomes with lysosomes.

To investigate a possible mechanism accounting for the reduced phago-lysosome fusion, we tracked single phagocytosed beads over long distances to analyze phagosomal motility, reflecting migration along cytoskeleton elements—most presumably along microtubules (Blocker et al., 1997). The results consistently showed that LAMP-1 recruitment to phagosomes was abolished in LPS-treated BMDCs bearing clustered lysosomes. On the contrary, in BMDCs displaying dispersed lysosomes, from either resting or LPS-treated conditions, LAMP-1 was rapidly and efficiently recruited to phagosomes with the same kinetics (Figure 4F). We found that in resting BMDCs, phagosomes migrated with a mean velocity of 0.88 ± 0.11 μm/min before fusion with lysosomes. Migration decreased significantly after fusion with lysosomes (to 0.47 ± 0.02 μm/min), both in resting and non-clustered LPS-treated BMDCs (Figure 4G). Displacement of phagosomes was strongly reduced (0.26 ± 0.02 μm/min) in LPS-treated BMDCs with clustered lysosomes (Figure 4F). These results establish a strong correlation between the distribution of lysosomes and their fusion with phagosomes. Together with the observation that phagosomes move very slowly in these cells, the results suggest that the lack of phago-lysosome fusion in maturing BMDCs could be due to the sequestration of lysosomes in a part of the cell that phagosomes cannot reach effectively.

Inhibition of Phago-Lysosome Fusion Is Specific to TLR Ligand-Mediated Stimulation

To investigate whether other stimuli that induce DC maturation also impair phago-lysosomal fusion and promote lysosome redistribution, we treated BMDCs with the TLR7 ligand R848 or the TLR9 ligand CpG for 16 hr. Both induced increased expression of activation markers, similar to LPS (Figure S5A). Phagosomal degradation of bbOVA was also delayed as compared to resting cells, but to a lower extent than in LPS-treated DCs (Figure S5B). R848 and CpG induced lysosomal accumulation in the peri-nuclear area (Figure S5C), which was also less pronounced than in LPS-treated BMDCs (Figure S5D). In contrast, treatment of DCs with TNF, a pro-inflammatory cytokine that also induced effective increased expression of activation markers (Figure S5E), did not have any impact on phagosomal antigen degradation (Figure S5F) or lysosomal clustering (Figure S5G). We also tested whether LPS induces similar effects in bone-marrow-derived macrophages. While a faint reduction in OVA degradation was detected, no clustering of lysosomes was evident after 16 hr of LPS treatment (data not shown). Therefore, reduced phago-lysosome fusion and lysosomal clustering are induced only by TLR engagement (and not by other DC activation agents) and selectively in DCs (and not in macrophages).

Rab34 Controls Peri-Nuclear Accumulation of Lysosomes, Delays Phagosome Maturation, and Induces Efficient Cross-Presentation

To gain further insight on the molecular mechanisms responsible for the reduction in phago-lysosome fusion in maturing DCs, we next examined the possible role of the GTPase Rab34. In macrophages, Rab34 is involved in the positioning of lysosomes in the

Table 1. Phagosomes of Resting DCs Are Enriched in Phago-lysosomal Fusion Markers

UniProt / SwissProt Accession	Gene Name	Protein Name	Fold Change (repl. 1)	Fold Change (repl. 2)	Peptides in Both Replicates
V-type proton ATPase complex					
Q9R1Q9	*Atp6ap1*	V-type proton ATPase subunit S1	2.27	2.33	2, 2
P51863	*Atp6v0d1*	V-type proton ATPase subunit d 1	2.21	2.15	4, 4
P50516	*Atp6v1a*	V-type proton ATPase catalytic subunit A	2.32	3.10	2, 4
P62814	*Atp6v1b2*	V-type proton ATPase subunit B	2.33	2.63	4, 7
Q9Z1G3	*Atp6v1c1*	V-type proton ATPase subunit C 1	2.66	2.81	7, 10
P50518	*Atp6v1e1*	V-type proton ATPase subunit E 1	2.44	2.64	4, 5
Q9D1K2	*Atp6v1f*	V-type proton ATPase subunit F	2.51	2.43	3, 3
Q9CR51	*Atp6v1g1*	V-type proton ATPase subunit G 1	2.02	2.63	2, 2
Q8BVE3	*Atp6v1h*	V-type proton ATPase subunit H	2.35	3.00	3, 4
Lysosomal and plasma membrane hydrolases					
P97449	*Anpep*	Aminopeptidase N	1.55	−1.06	3, 2
P50429	*Arsb*	Arylsulfatase B	3.00	2.96	1, 2
Q9WV54	*Asah1*	Acid ceramidase	2.95	2.38	1, 5
P41731	*Cd63*	CD63 antigen	3.12	2.48	2, 2
P10605	*Ctsb*	Cathepsin B	2.46	4.88	2, 2
P18242	*Ctsd*	Cathepsin D	3.52	3.89	6, 8
P56542	*Dnase2*	Deoxyribonuclease-2-alpha	3.70	6.13	3, 2
Q9Z0L8	*Ggh*	Gamma-glutamyl hydrolase	2.02	3.10	2, 3
P51569	*Gla*	Alpha-galactosidase A	3.91	4.19	2, 1
Q60648	*Gm2a*	Ganglioside GM2 activator	1.97	7.24	2, 2
P12265	*Gusb*	Beta-glucuronidase	2.33	5.36	6, 4
P29416	*Hexa*	Beta-hexosaminidase subunit alpha	2.26	2.24	2, 1
P20060	*Hexb*	Beta-hexosaminidase subunit beta	2.55	1.75	3, 1
P11438	*Lamp1*	Lysosome-associated membrane glycoprotein 1	2.87	2.52	3, 3
P17047	*Lamp2*	Lysosome-associated membrane glycoprotein 2	2.41	1.83	3, 3
Q9Z0M5	*Lipa*	Lysosomal acid lipase hydrolase	2.75	3.09	2, 3
O09159	*Man2b1*	Lysosomal alpha-mannosidase	3.39	3.82	2, 1
Q7TMR0	*Prcp*	Lysosomal Pro-X carboxypeptidase	2.12	6.98	2, 2
Q61207	*Psap*	Sulfated glycoprotein 1	3.09	4.12	4, 5
Q920A5	*Scpep1*	Retinoid-inducible serine carboxypeptidase	1.53	5.25	2, 2
P58242	*Smpdl3b*	Acid sphingomyelinase-like phosphodiesterase 3b	2.07	−1.18	2, 2
Q9JJF9	*Sppl2a*	Signal peptide peptidase-like 2A	1.38	1.36	1, 2
Fusion and vesicular trafficking					
O35643	*Ap1b1*	AP-1 complex subunit beta-1	−1.25	1.25	3, 1
Q9Z1T1	*Ap3b1*	AP-3 complex subunit beta-1	−1.27	−1.50	2, 1
Q9D8B3	*Chmp4b*	Charged multivesicular body protein 4b	−1.26	−1.45	4, 2
O08917	*Flot1*	Flotillin-1	1.84	2.34	4, 7
Q60634	*Flot2*	Flotillin-2	1.74	2.75	2, 5
Q61598	*Gdi2*	Rab GDP dissociation inhibitor beta	−1.12	1.72	3, 5
P62821	*Rab1a*	Ras-related protein Rab-1A	1.15	1.22	3, 4
Q9D1G1	*Rab1b*	Ras-related protein Rab-1B	1.09	1.20	5, 7
P53994	*Rab2a*	Ras-related protein Rab-2A	1.14	1.44	2, 3
P35278	*Rab5c*	Ras-related protein Rab-5C	1.24	1.74	1, 5
P35279	*Rab6a*	Ras-related protein Rab-6A	−1.07	1.02	1, 3
P51150	*Rab7a*	Ras-related protein Rab-7A	1.22	1.74	5, 7
P61028	*Rab8b*	Ras-related protein Rab-8B	1.34	1.37	2, 1
Q9R0M6	*Rab9a*	Ras-related protein Rab-9A	1.30	1.95	1, 2

(*Continued on next page*)

Table 1. *Continued*

UniProt / SwissProt Accession	Gene Name	Protein Name	Fold Change (repl. 1)	Fold Change (repl. 2)	Peptides in Both Replicates
P46638	*Rab11b*	Ras-related protein Rab-11B	1.15	1.23	2, 1
Q91V41	*Rab14*	Ras-related protein Rab-14	1.13	1.66	3, 4
P35293	*Rab18*	Ras-related protein Rab-18	1.00	1.32	2, 2
Q9ERI2	*Rab27a*	Ras-related protein Rab-27A	1.15	−1.08	2, 2
O09044	*Snap23*	Synaptosomal-associated protein 23	−1.10	−1.41	2, 2
O70492	*Snx3*	Sorting nexin-3	1.19	1.79	1, 3
Q9D8U8	*Snx5*	Sorting nexin-5	−1.20	1.24	1, 2
Q64704	*Stx3*	Syntaxin-3	−1.17	−1.48	2, 3
O70439	*Stx7*	Syntaxin-7	1.63	1.30	2, 2
Q9QZ88	*Vps29*	Vacuolar protein sorting-associated protein 29	1.45	2.01	2, 2
Q9EQH3	*Vps35*	Vacuolar protein sorting-associated protein 35	1.31	1.70	3, 3
P46467	*Vps4b*	Vacuolar protein sorting-associated protein 4B	1.76	−1.09	4, 3
O88384	*Vti1b*	Vesicle transport through interaction with t-SNAREs 1B	1.15	1.86	1, 2
Proteasomal degradation					
Q9R1P4	*Psma1*	Proteasome subunit alpha type-1	1.02	1.43	2, 1
Q9R1P0	*Psma4*	Proteasome subunit alpha type-4	−1.04	1.40	3, 2
Q9Z2U1	*Psma5*	Proteasome subunit alpha type-5	1.02	1.41	2, 2
Q9Z2U0	*Psma7*	Proteasome subunit alpha type-7	−1.09	1.01	4, 1
P46471	*Psmc2*	26S protease regulatory subunit 7	−1.32	3.07	2, 1
P97371	*Psme1*	Proteasome activator complex subunit 1	−1.44	−1.16	3, 3
ER-associated proteins					
O55143	*Atp2a2*	SR/ER calcium ATPase 2	1.15	−1.13	7, 3
Q64518	*Atp2a3*	SR/ER calcium ATPase 3	−1.21	−1.34	3, 2
P14211	*Calr*	Calreticulin	1.11	−1.23	6, 9
P35564	*Canx*	Calnexin	1.17	−1.40	6, 13
P57759	*Erp29*	ER resident protein 29	−1.01	−1.19	4, 6
Q9D1Q6	*Erp44*	ER resident protein 44	1.00	−1.06	1, 3
P07901	*Hsp90aa1*	Heat shock protein HSP 90-alpha	−1.27	−1.01	4, 6
P11499	*Hsp90ab1*	Heat shock protein HSP 90-beta	−1.40	−1.13	2, 3
Q61316	*Hspa4*	Heat shock 70 kDa protein 4	1.10	1.41	6, 2
P20029	*Hspa5*	78 kDa glucose-regulated protein	−1.13	−1.29	9, 15
P63017	*Hspa8*	Heat shock cognate 71 kDa protein	1.06	1.22	9, 10
P09103	*P4hb (Pdia1)*	Protein disulfide-isomerase	1.08	−1.09	10, 13
P27773	*Pdia3*	Protein disulfide-isomerase A3	−1.09	−1.25	9, 8
P08003	*Pdia4*	Protein disulfide-isomerase A4	1.03	−1.10	13, 15
Q922R8	*Pdia6*	Protein disulfide-isomerase A6	1.10	−1.17	4, 4
Q01853	*Vcp*	Transitional endoplasmic reticulum ATPase	1.24	1.03	4, 3

Phagosomes containing bbOVA were isolated from resting and LPS-treated BMDCs after 30 min pulse and 60 min chase. After lysis and precipitation, samples were labeled with $^{12}C_3$- (resting cells) and $^{13}C_3$-propionate (LPS-treated cells), equal amounts were mixed and analyzed by LC-MS/MS. Shown are functional categories of proteins that were identified in two independent experiments (repl. 1 and 2) including their fold change. Values above 2.02 (repl. 1) and 2.67 (repl. 2) represent enrichment in phagosomes of resting DCs, while values below −1.52 (repl. 1) and −1.63 (repl. 2) show enrichment in phagosomes of LPS-treated DCs. See also Figure S4.

peri-nuclear region (Wang and Hong, 2002). Rab34 also has a role in the transport of lysosomal cargo to phagosomes (Kasmapour et al., 2012) and was proposed to play a role in cross-presentation, based on siRNA screening (Zou et al., 2009). We used siRNA-mediated gene silencing to decrease expression of *Rab34*. Transfection did not alter the phenotype of BMDCs, which responded normally to LPS (Figures S6A and S6B). Rab34 expression was analyzed by Western blotting (Figures 5A and S6C). Four different siRNA inhibited Rab34 expression with varying efficiencies as compared to the control (Figure S6C). siRNA #4 was the most efficient at silencing Rab34. Silenced *Rab34* did not affect the kinetics of phago-lysosome fusion in resting BMDCs (Figures 5B and 5C). In contrast, in *Rab34* silenced BMDCs we failed to observe any LPS-induced delay in OVA degradation or phago-lysosome fusion (Figures 5B and 5C). This effect was confirmed using *Rab34* siRNA #1, which

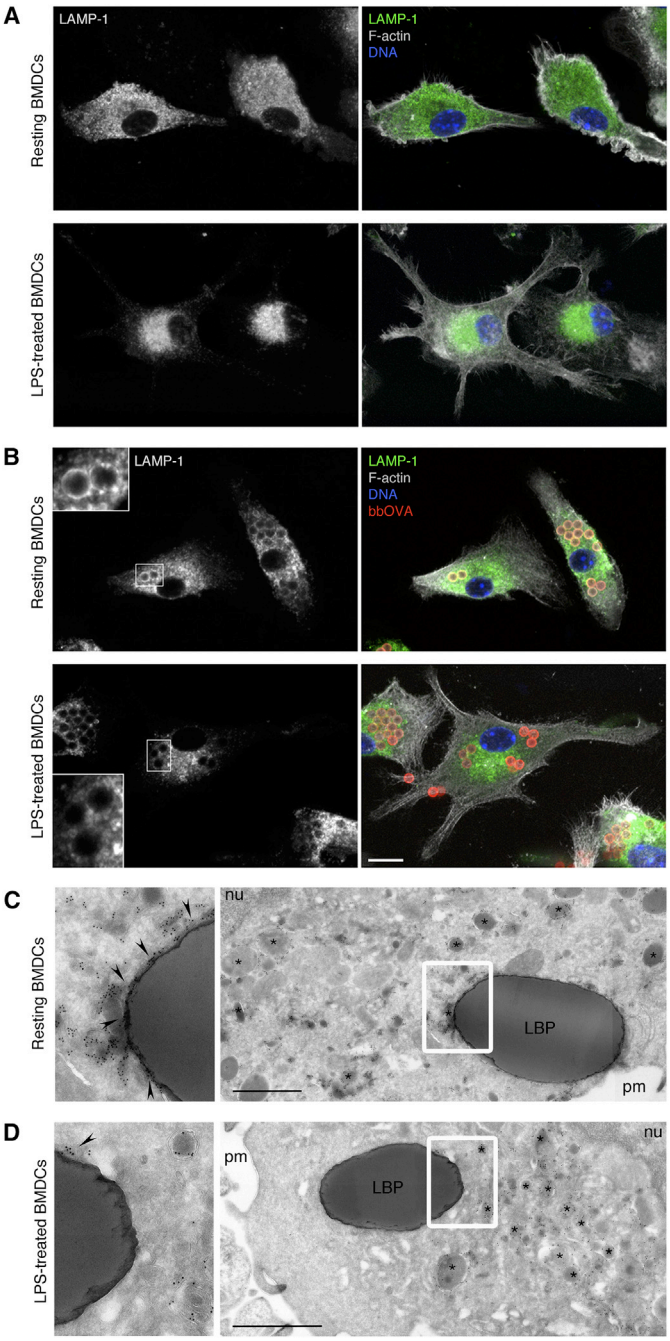

Figure 3. Lysosomal Compartments of LPS-Treated DCs Display Peri-nuclear Clustering

BMDCs were grown in absence (resting) or presence of 100 ng/ml LPS (LPS-treated), labeled, and analyzed by confocal microscopy.

(A) Shown are projections of stainings of LAMP-1 (green), F-actin (gray), and DNA (blue).

(B) The same cells were allowed to internalize bbOVA for 30 min followed by a chase period of 60 min. In merged images, LAMP-1 (green), F-actin (gray), DNA (blue), and bbOVA (red) are shown. Insets display phagosomes of both cell types.

(C and D) Electron microscopy of resting (C) and LPS-treated BMDCs (D) after labeling of LAMP-1 with 10 nm gold.

(E) Quantification of gold particles per phagosome area after 0 min and 60 min phagosome maturation. At least 60 phagosomes from three independent experiments for each condition were measured. Error bars represent SD. Scale bars represent 10 µm (A and B) and 1 µm (C and D), respectively.

has a partial effect on both *Rab34* silencing and the reversion of the LPS-induced reduction in phago-lysosome fusion (Figures S6D and S6E). These results show that Rab34 expression is dispensable for phago-lysosome fusion in resting BMDCs but is required for the reduction of phago-lysosome fusion induced by LPS.

Because of the correlation between lysosome clustering and fusion with phagosomes, we analyzed the effect of *Rab34* silencing on lysosome distribution in resting and LPS-treated BMDCs (Figures 6A and 6B). Silenced *Rab34* did not affect the disperse distribution of lysosomes in resting BMDCs (Figure 6A). In contrast, *Rab34* silencing prevented the induction of lysosome clustering by LPS (Figure 6B). Single cell analysis was performed to quantify the subcellular distribution of lysosomes in control and *Rab34* silenced BMDCs, as described above. While resting cells transfected with control siRNA had a lysosomal relative area between 0.5 and 0.8 (characteristic for a wide peripheral distribution of lysosomes) in approximately 35%–40% of LPS-treated control cells the lysosomal relative area value was reduced to 0.1–0.4 (corresponding to the clustering of lysosomes; Figure 6C). These results show that *Rab34* silenced BMDCs lose their ability to cluster lysosomes after activation with LPS.

Finally, we tested whether silencing of *Rab34* also prevents the increase in cross-presentation efficiency induced by LPS. The processed SIINFEKL peptide was used as a control for cross-presentation, which did not exhibit differences between the different samples. In cells transfected with control siRNA, LPS treatment increased the efficiency of cross-presentation for both bbOVA and sOVA (Figure 6D). In contrast, in *Rab34* silenced BMDCs LPS failed to induce any significant increase in the efficiency of OVA cross-presentation (Figure 6E). Therefore, expression of Rab34 is required for the increase in the efficiency of cross-presentation observed after 16 hr of LPS stimulation.

DISCUSSION

Lysosome clustering during DC maturation was observed over 15 years ago (Pierre et al., 1997), but its functional relevance

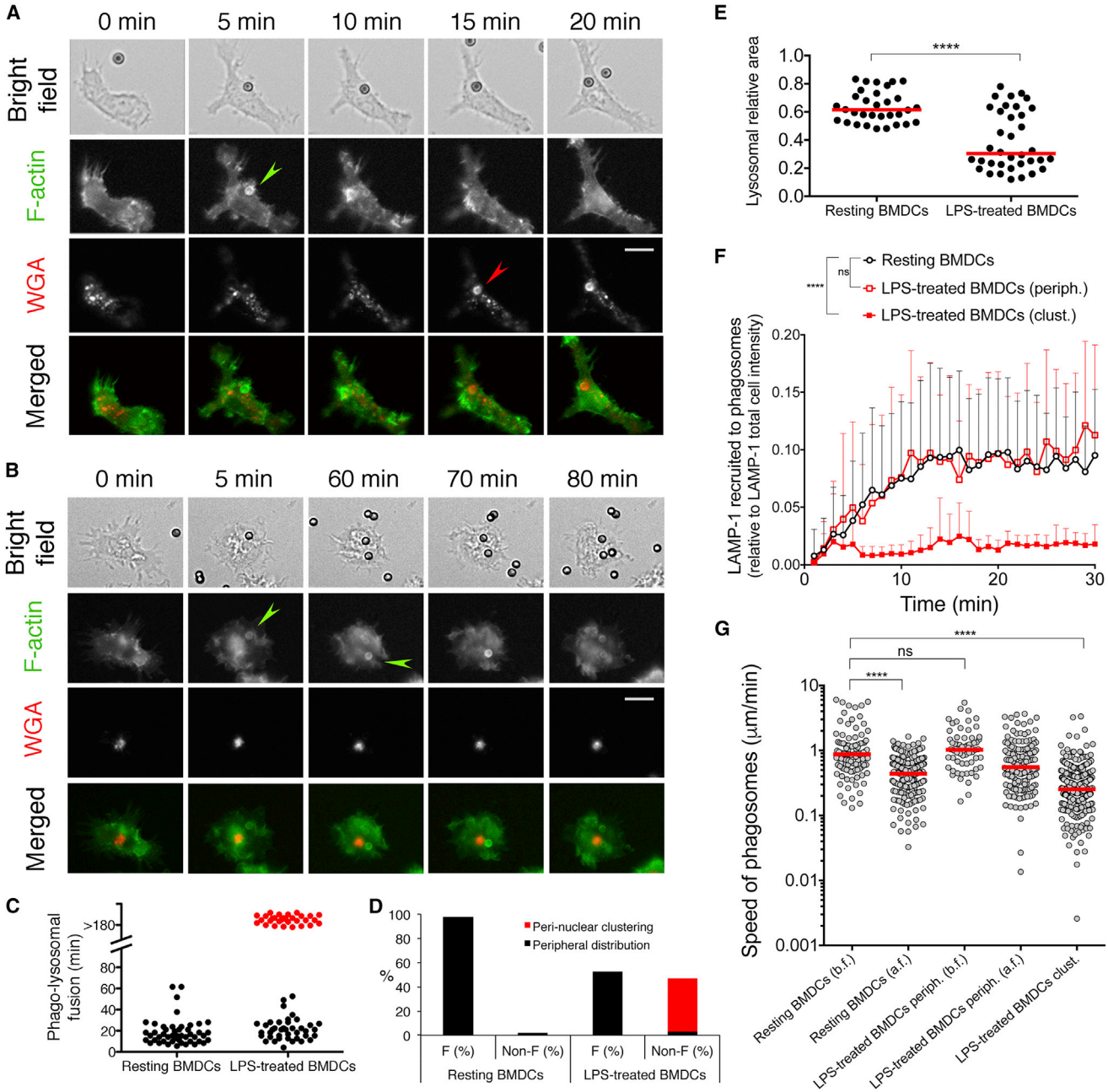

Figure 4. DCs with Peri-nuclear Clustering of Lysosomes Are Strongly Reduced in Phago-lysosomal Fusion

BMDCs expressing LifeAct-GFP (green) were pre-incubated with fluorescently-labeled WGA that accumulates in lysosomes (red). After lysosomal loading, bbOVA was added and phagocytic uptake (green arrows) and phago-lysosomal (P-L) fusion (red arrow) were analyzed by video microscopy in resting (A) and LPS-treated BMDCs (B). P-L fusion kinetics were quantified in both cell types (C) as well as percentages of DCs with peripheral distribution of lysosomes (black) or peri-nuclear clustering of lysosomes (red) 180 min after addition of beads (D). Additionally, DCs were also sub-divided in cells that contained fused (F) and non-fused (non-F) phagosomes. Clustering of lysosomes in non-treated and LPS-treated BMDCs was measured; intracellular areas of DCs were quantified for their relative LAMP-1$^+$ areas (cell number > 30 for each analyzed condition) (E). Recruitment of LAMP-1 to phagosomes was evaluated by tracking each phagosome individually; average of all phagosomes for each condition is graphed (periph.: peripheral distribution of lysosomes; clust.: lysosomes clustered in the peri-nuclear region) (F). Migration speed of phagosomes along microtubules was quantified; b.f. = before fusion of phagosomes and lysosomes, a.f. = after fusion (G). Shown is a representative example of two independent experiments. Error bars represent SD. Scale bars represent 10 μm. See also Movies S1 and S2 and Figures S3 and S5.

was unknown until the present study. Our findings suggest that perinuclear clustering of lysosomes in maturing DCs, together with reduced displacements of phagosomes along microtubules, prevent effective phago-lysosome fusion, thereby promoting antigen cross-presentation. This conclusion is based on the following observations. First, within a heterogeneous

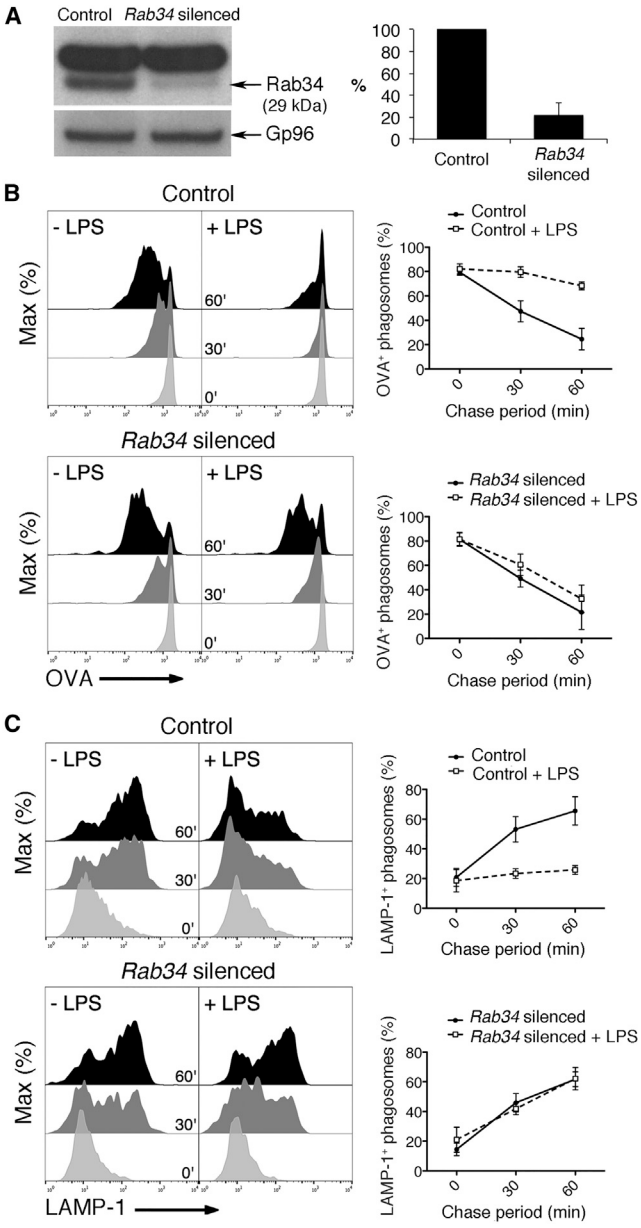

Figure 5. Silencing of *Rab34* Reverts Delayed Phagosome Maturation in LPS-Treated DCs

BMDCs were transfected with scramble siRNA (control) and *Rab34* siRNA #4 (*Rab34* silenced). Efficiency of silencing was tested and quantified by Western blotting (A). BMDCs were incubated for 16 hr in presence or absence of 100 ng/ml LPS before bbOVA was phagocytosed. Phagosomal degradation of OVA (B) as well as phagosomal acquisition of LAMP-1 (C) were analyzed after different chase periods by flow organellocytometry. Shown are representative data of three independent experiments. Error bars represent SD. See also Figure S6.

population of maturing DCs, including cells bearing non-clustered and clustered lysosomes, there was a strict negative correlation between lysosomal clustering and phago-lysosome fusion. Second, silencing of *Rab34* prevented both lysosomal clustering and the inhibition of phago-lysosome fusion induced by LPS, without affecting phagosomal maturation or lysosomal distribution in resting BMDCs. Finally, the observation that silencing of *Rab34* also prevented the increased efficiency of cross-presentation induced by LPS, but does not affect cross-presentation in untreated BMDCs, indicates that reducing the fusion of phagosomes and lysosomes plays a critical role in the increased efficiency of cross-presentation by maturing DCs. Together, these results suggest that DCs have developed a dedicated mode of control of phago-lysosomal fusion, based on a Rab34-dependent re-organization of the intracellular distribution of lysosomes, that transiently promotes the efficiency of cross-presentation in maturing DCs.

The innate response of DCs to pathogens includes a series of developmentally controlled changes of cellular morphology and function. Many of these changes relate to antigen presentation and T cell activation (Reis e Sousa, 2006). The inhibition of phago-lysosome fusion reported here starts only around 12 hr after TLR4 engagement. It is assumed, however, that in most cases antigen and TLR ligands are encountered and phagocytosed simultaneously. What is the physiological relevance of the process that we are reporting here? There are several possible answers to this question. First, although a single bacterium might bear sufficient LPS to activate a DC, it might not contain sufficient antigen to induce effective priming. Our results predict that activated DCs enter a "surveillance" state that allows uptake of additional microbes (as the infection develops and more microbes become available) and efficient cross-presentation for up to 16–18 hr after TLR engagement, even if the precise kinetics of this transient phase can change depending on the concentration and purity of the LPS preparations and the type of DCs analyzed. It is also possible that in the course of infections, pathogens or infected cells produce soluble TLR ligands that "prime" DCs locally several hours before the actual microbe is encountered and taken up. Finally, the idea of a TLR ligand-induced phase of increased cross-presentation is consistent with the notion that DCs need to take up and cross-present antigens while pathogens are present, but before tissue destruction becomes too important, thus avoiding the uptake of self-antigens and their cross-presentation, which could represent a potential danger due to self-reactivity.

A recent study from the Villadangos group has shown that DCs activated in vivo by CpG for 12 hr fail to cross-present antigen from dead cells, while "indirectly" activated DCs (i.e., TLR-deficient DCs activated by secreted cytokines in a wild-type context) could take up and cross-present antigen after activation (Vega-Ramos et al., 2014). Consistent with these results, 16 hr after injection of LPS, DCs failed to take up dead cells or cross-present antigen from dead cell-OVA in vivo (data not shown). These results indicate that the mechanism reported here is not relevant for antigens expressed in dying non-infected cells, consistent with the idea that early after activation DCs focus their uptake and antigen presentation capacity on non-self antigen sources. In our in vitro experiments, TNF, an inflammatory cytokine that effectively activates DCs and is produced by different phagocytes in response to TLR engagement, did not induce a phago-lysosome block or lysosomal clustering. Although "indirectly" activated DCs do not present antigen to $CD4^+$ T cells (Spörri and Reis e Sousa, 2005), it is still unclear whether they are competent for cross-presentation (Kratky et al., 2011; Vega-Ramos et al., 2014). Depending on the experimental

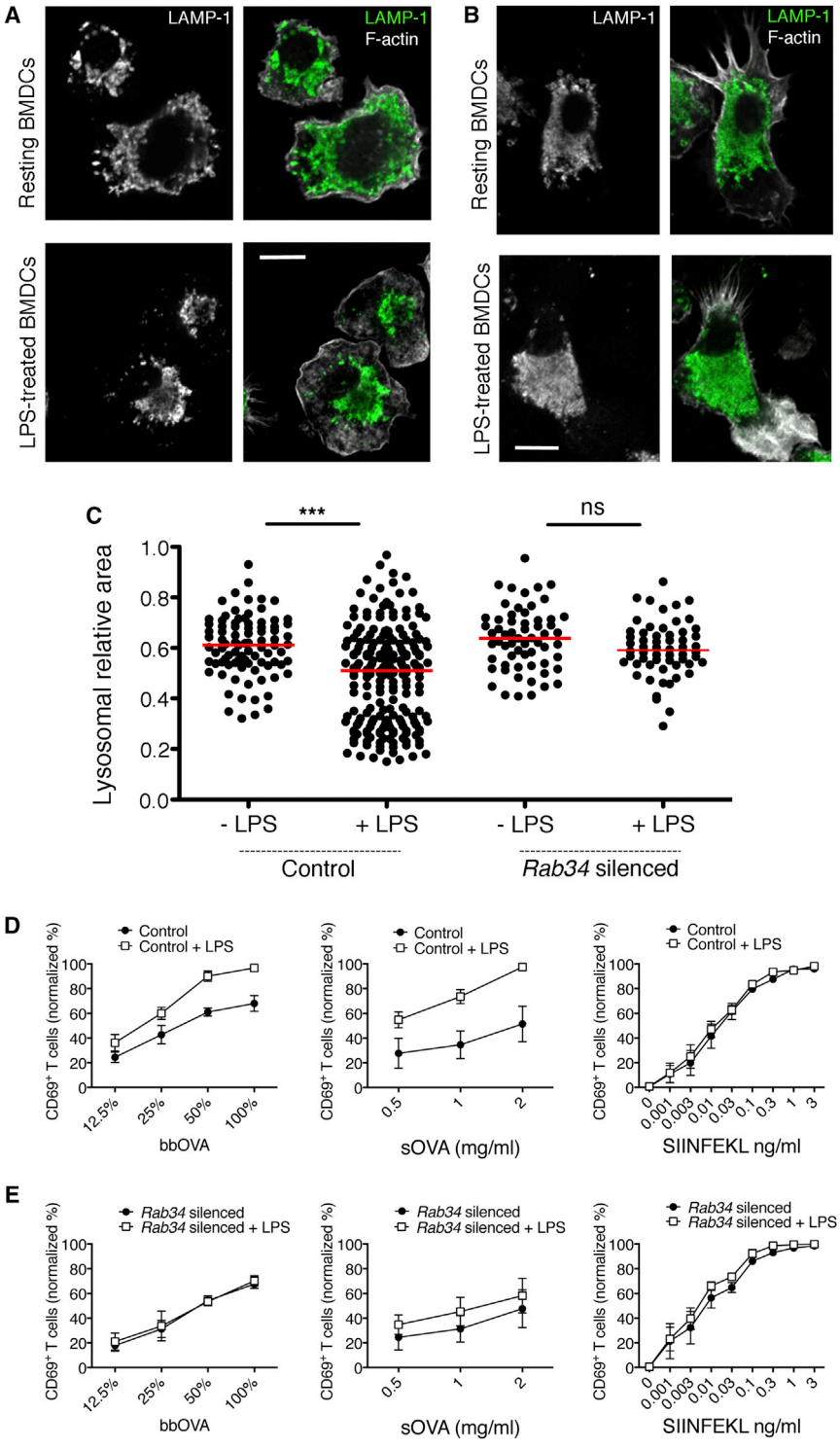

Figure 6. Silencing of Rab34 Reduces Efficient Cross-Presentation in LPS-Treated DCs

BMDCs transfected with scramble siRNA (control) and *Rab34* siRNA #4 (*Rab34* silenced) were labeled and analyzed by confocal microscopy. Shown are projections of stainings of LAMP-1 (green) and F-actin (gray) of control (A) and *Rab34* silenced BMDCs (B) before and after LPS treatment. Intracellular areas of DCs were quantified for their relative LAMP-1+ areas (cell number > 80 for each analyzed condition) (C). The same cells were also analyzed for cross-presentation of bbOVA (left panel), sOVA (middle panel), and SIINFEKL peptide (right panel) measured by CD69 expression of OT-I T cells co-cultured with control (D) and *Rab34* silenced BMDCs (E) in presence and absence of LPS. Shown are normalized data of three independent experiments. Scale bars represent 10 μm. See also Figure S6.

systems (including kinetics, amounts of antigen and nature of TLR ligands), the block in phago-lysosome fusion described herein may or may not operate. It is also possible, however, that "indirectly" in vivo activated DCs receive a combination of innate signals, in addition to TNF, that induce lysosomal clustering and inhibit phago-lysosome fusion in vivo. Finally, the phenomenon that we describe here could also be relevant to DCs in mucosae, which are constantly stimulated by TLR ligands from microbiota or to infection-related autoimmunity, during which TLR engagement could promote the cross-presentation of self-antigens.

Although it was unexpected that maturing DCs failed to fuse phagosomes to lysosomes, it is not unexpected that such a block results in enhanced cross-presentation in DCs. Abundant previous evidence by others and us, suggest that decreased phagosome cargo degradation favors cross-presentation (Graham et al., 2007; Jancic et al., 2007; Mantegazza et al., 2008; Savina et al., 2006, 2009). Slow degradation probably spares MHC I-restricted epitopes in the endocytic pathway, and allows effective export to the cytosol of large protein fragments that can be processed by the proteasome. Of note, the increased efficacy of cross-presentation reported here occurs while the efficiency of phagocytosis is progressively reduced, suggesting that maturing DCs, even if they cross-present antigens more efficiently, take up less antigen by phagocytosis, which most likely participates to reducing antigen presentation by MHC II during this transient phase. Slow internalization has indeed previously been shown to favor cross-presentation in human DCs, after targeting of antigens to relatively inefficient endocytic receptors, such as CD40 (Hoffmann et al., 2001).

Although the present study identifies a mechanism that is turned on several hours after DC activation by TLR engagement, upregulation of cross-presentation starts as soon as a TLR ligand-bearing particle is taken up. We and others have shown

previously that when DCs encounter antigen and TLR ligands simultaneously, cross-presentation is increased (Nair-Gupta et al., 2014). The mechanisms involved in this early (first few hours) increase in cross-presentation have been investigated in many studies: Increased recruitment of MHC I to phagosomes (Nair-Gupta et al., 2014), decreased recruitment of lysosomal enzymes (Delamarre et al., 2005), and higher pH (Savina et al., 2006) have all been proposed to participate to increased cross-presentation in the first few hours after antigen uptake.

It has also been reported that during late phases of DC maturation in response to LPS and other TLR ligands that cross-presentation is down-modulated (Gil-Torregrosa et al., 2004; Wagner and Cresswell, 2012; Samie and Cresswell, 2015). Our earlier study showed that after 24–30 hr of LPS stimulation DCs fail to cross-present antigen, probably due to reduced antigen export to the cytosol (Gil-Torregrosa et al., 2004). More recently, Cresswell and colleagues showed that down-modulation of cross-presentation is induced by peptidoglycan contaminating some LPS preparations and also by high doses of pure LPS (Wagner and Cresswell, 2012). They also showed that TFEB coordinates the selective down-modulation of antigen cross-presentation at these late times (24 hr) after LPS-mediated stimulation by promoting endosomal acidification and antigen degradation (Samie and Cresswell, 2015). These studies, however, did not investigate the transient phase of induction of cross-presentation, but since TFEB promotes phagosomal acidification during late phases of DC maturation, it is probably not involved in the transient increase of cross-presentation analyzed here.

We propose that the Rab34-dependent block in phagolysosome fusion is a mechanism for this intermediate phase of prolonged enhancement of antigen cross-presentation. The generation of conditional *Rab34*$^{-/-}$ mice will allow addressing the exact role of increased antigen cross-presentation by TLR ligand engagement for CD8$^+$ T cell responses to pathogens and tumors. Our findings, nevertheless, should help designing more effective CD8$^+$ T cell vaccination strategies.

EXPERIMENTAL PROCEDURES

Cell Generation

C57BL/6 female mice and C57BL/6 TCR (Vα2, Vβ5) transgenic mice (OT-I) were obtained from Charles River Laboratories, Janvier, and CDTA. All animal procedures were in accordance with the guidelines and regulations of the French Veterinary Department or were approved by the animal ethical committee of Ghent University, Belgium. BMDCs and splenic DCs were generated by culture in GM-CSF-containing medium. In vitro maturation of cells was induced by a 16 hr treatment with 100 ng/ml of ultrapure LPS from *E. coli* 0111:B4 (Invivogen) unless otherwise stated. For full information on mice, cells and antibodies, see Supplemental Experimental Procedures.

Bead Preparation

Amine-modified polystyrene beads (Polysciences) were pre-activated with 8% (vol/vol) glutaraldehyde for 4 hr at room temperature. Beads were conjugated to low endo ovalbumin (Worthington Biochemicals) and Alexa Fluor N-hydroxysuccinimide ester dyes (Life Technologies) on a rotating wheel overnight at 4°C at concentrations of 0.5 mg/ml and 0.1 mg/ml, respectively. After quenching in PBS containing 0.5 M glycine for 30 min, beads were used for phagocytosis assays.

As for the in vivo cross-presentation experiments, polybeads (Polysciences) were coated with 20 mg/ml soluble OVA overnight and washed three times with PBS before injection.

Flow Organellocytometry

The flow cytometry techniques used to analyze the capacity of phagosomes to degrade proteins and acquire LAMP-1 have been described previously (Savina et al., 2010). In brief, after phagocytic uptake of bead-bound OVA, cells were washed in cold PBS and non-specific binding sites were blocked by incubation with CD16/32 antibody (BD Biosciences). Subsequently, in all samples, external beads were labeled and excluded from analysis. Samples were resuspended in homogenization buffer and disrupted mechanically with 2 ml syringes and 22-gauge needles (Terumo Medical). After centrifugation, the post-nuclear supernatant was transferred to 96-well conical microplates followed by labeling on ice using antibodies against OVA, LAMP-1, and LAMP-2. Samples were measured by flow cytometry using the LSR II cytometer (BD Biosciences) and analyzed by FlowJo software (TreeStar).

In Vitro Cross-Presentation Assays

BMDCs were incubated with bbOVA, with sOVA, or with different concentrations of the SIINFEKL peptide. After 1 hr, DCs were washed and co-cultured with purified CFSE-OT-I CD8$^+$ T cells for 3 days. To evaluate T cell proliferation, diminution of CFSE staining on the TCR$^+$ CD8$^+$ population was measured by flow cytometry. Alternatively, cells were incubated for 5 hr with the same antigens. Then, cells were fixed with 0.008% glutaraldehyde in PBS. Cross-presentation was analyzed either by co-culturing with B3Z cells for 16 hr (detecting β-galactosidase activity by optical density at 590 nm using CPRG as substrate) or by co-culturing with OT-I CD8$^+$ T cells (activation was measured after 16 hr by expression of CD69).

In Vivo Maturation of DCs and Cross-Presentation Assays

A dose of 10 μg LPS (ultrapure, *E. coli* 0111:B4, Invivogen) was chosen to generate maximum numbers of activated DCs judged by upregulation of co-stimulatory molecules (CD40, CD86), but the lowest associated pathology. Endotoxin-free PBS was used for control injections. For bbOVA, LPS was injected intraperitoneally 14 hr prior to experiments, followed by intravenous injection of beads and 2 hr of phagocytosis. Subsequently, spleens were harvested and DCs were purified by CD11c negative selection (Miltenyi) followed by sorting CD8$^+$ bead$^+$ DCs. For sOVA and OVA-IC, LPS was injected 15.5 hr prior to experiments, and the antigen was administered i.v. for 30 min. Again, spleens were collected, followed by two rounds of CD11c negative selection. DCs were then co-cultured with OT-I T cells for 16 hr and activation of T cells was addressed by CD25 and CD69 expression.

siRNA-Mediated *Rab34* Gene Silencing

BMDC transfection was performed by electroporation with 4 different siRNA following the manufacturer's instructions (Amaxa) with some minor modifications. Briefly, BMDCs were harvested at day 7 and resuspended in the electroporation solution provided with the kit. 2×10^6 cells were distributed per cuvette and electroporated. Cells were quickly plated back in 6-well plates with 3 ml of complete medium. After 24 hr, the medium was replaced by fresh medium. After 48 hr, cells were harvested and analyzed (for sequences and details, see Supplemental Experimental Procedures).

SUPPLEMENTAL INFORMATION

Supplemental Information includes six figures, Supplemental Experimental Procedures, and two movies and can be found with this article online at http://dx.doi.org/10.1016/j.immuni.2015.11.006.

AUTHOR CONTRIBUTIONS

Conceptualization by A.A., F.K., A.S., E.H., and S.A.; Investigation by A.A., F.K., A.-M.P., J.-M.C., M.J., E.T., L.P., P.V., U.G., L.J., O.I.V., and E.H.; Resources from A.-M.L.-D., and K.G.; Formal analysis by A.A., J.-M.C., E.T., M.M., and K.G.; Funding acquisition by R.B., E.H., and S.A.; Writing by A.A., F.K., E.H., and S.A.; Supervision by R.B., E.H., and S.A.

ACKNOWLEDGMENTS

We are grateful to J. Magalhaes, A. Zamaleeva, A. Goncalves, G. Van Isterdael for technical assistance and B. Lambrecht, H. Hammad, M. Guillams for

scientific discussions. We acknowledge the PICT-IBiSA@Pasteur microscopy facility (Institute Curie, Paris), the Bio Imaging Core (VIB, Ghent), and the flow cytometry facilities at Institute Curie and the IRC. This work was supported by the French National Research Agency through the "Investments for the Future" program (France-BioImaging, ANR-10-INSB-04), ANR-11-LABX-0043 and by the CelTisPhyBio Labex (N° ANR-10-LBX-0038), part of the IDEX PSL (ANR-10-IDEX-0001-02 PSL). We are grateful to the financial support by the European Research Council (2013-AdG N° 340046 DCBIOX), La Ligue Nationale contre le Cancer (EL2014.LNCC/SA), Fonds Wetenschappelijk Onderzoek (FWO), the "Interuniversity Attraction Poles" (IAP7), Ghent University "Concerted Research Actions" (GOA) and "Group-ID MRP." A.A. was supported by an EMBO long-term fellowship (ALTF 883-2011), A.-M.P. by an FWO fellowship (11W8415N), J.-M.C. by a fellowship of La Ligue contre le Cancer, and E.H. by fellowships of Fondation Recherche Médicale (SPF20101221176), the omics@VIB program (co-financed by the Marie Curie FP7 People Cofund) and an FWO grant (1526615N).

Received: February 22, 2015
Revised: August 15, 2015
Accepted: November 5, 2015
Published: December 15, 2015

REFERENCES

Blander, J.M., and Medzhitov, R. (2006). Toll-dependent selection of microbial antigens for presentation by dendritic cells. Nature *440*, 808–812.

Blocker, A., Severin, F.F., Burkhardt, J.K., Bingham, J.B., Yu, H., Olivo, J.C., Schroer, T.A., Hyman, A.A., and Griffiths, G. (1997). Molecular requirements for bi-directional movement of phagosomes along microtubules. J. Cell Biol. *137*, 113–129.

Cebrian, I., Visentin, G., Blanchard, N., Jouve, M., Bobard, A., Moita, C., Enninga, J., Moita, L.F., Amigorena, S., and Savina, A. (2011). Sec22b regulates phagosomal maturation and antigen crosspresentation by dendritic cells. Cell *147*, 1355–1368.

Delamarre, L., Pack, M., Chang, H., Mellman, I., and Trombetta, E.S. (2005). Differential lysosomal proteolysis in antigen-presenting cells determines antigen fate. Science *307*, 1630–1634.

Flannagan, R.S., Cosío, G., and Grinstein, S. (2009). Antimicrobial mechanisms of phagocytes and bacterial evasion strategies. Nat. Rev. Microbiol. *7*, 355–366.

Gil-Torregrosa, B.C., Lennon-Duménil, A.M., Kessler, B., Guermonprez, P., Ploegh, H.L., Fruci, D., van Endert, P., and Amigorena, S. (2004). Control of cross-presentation during dendritic cell maturation. Eur. J. Immunol. *34*, 398–407.

Graham, D.B., Stephenson, L.M., Lam, S.K., Brim, K., Lee, H.M., Bautista, J., Gilfillan, S., Akilesh, S., Fujikawa, K., and Swat, W. (2007). An ITAM-signaling pathway controls cross-presentation of particulate but not soluble antigens in dendritic cells. J. Exp. Med. *204*, 2889–2897.

Guermonprez, P., Saveanu, L., Kleijmeer, M., Davoust, J., Van Endert, P., and Amigorena, S. (2003). ER-phagosome fusion defines an MHC class I cross-presentation compartment in dendritic cells. Nature *425*, 397–402.

Hoffmann, T.K., Meidenbauer, N., Müller-Berghaus, J., Storkus, W.J., and Whiteside, T.L. (2001). Proinflammatory cytokines and CD40 ligand enhance cross-presentation and cross-priming capability of human dendritic cells internalizing apoptotic cancer cells. J. Immunother. *24*, 162–171.

Inaba, K., Turley, S., Iyoda, T., Yamaide, F., Shimoyama, S., Reis e Sousa, C., Germain, R.N., Mellman, I., and Steinman, R.M. (2000). The formation of immunogenic major histocompatibility complex class II-peptide ligands in lysosomal compartments of dendritic cells is regulated by inflammatory stimuli. J. Exp. Med. *191*, 927–936.

Jancic, C., Savina, A., Wasmeier, C., Tolmachova, T., El-Benna, J., Dang, P.M.-C., Pascolo, S., Gougerot-Pocidalo, M.-A., Raposo, G., Seabra, M.C., and Amigorena, S. (2007). Rab27a regulates phagosomal pH and NADPH oxidase recruitment to dendritic cell phagosomes. Nat. Cell Biol. *9*, 367–378.

Joffre, O.P., Segura, E., Savina, A., and Amigorena, S. (2012). Cross-presentation by dendritic cells. Nat. Rev. Immunol. *12*, 557–569.

Kasmapour, B., Gronow, A., Bleck, C.K.E., Hong, W., and Gutierrez, M.G. (2012). Size-dependent mechanism of cargo sorting during lysosome-phagosome fusion is controlled by Rab34. Proc. Natl. Acad. Sci. USA *109*, 20485–20490.

Kinchen, J.M., and Ravichandran, K.S. (2008). Phagosome maturation: going through the acid test. Nat. Rev. Mol. Cell Biol. *9*, 781–795.

Kratky, W., Reis e Sousa, C., Oxenius, A., and Spörri, R. (2011). Direct activation of antigen-presenting cells is required for CD8+ T-cell priming and tumor vaccination. Proc. Natl. Acad. Sci. USA *108*, 17414–17419.

Kurts, C., Heath, W.R., Carbone, F.R., Allison, J., Miller, J.F., and Kosaka, H. (1996). Constitutive class I-restricted exogenous presentation of self antigens in vivo. J. Exp. Med. *184*, 923–930.

Lennon-Duménil, A.-M., Bakker, A.H., Maehr, R., Fiebiger, E., Overkleeft, H.S., Rosemblatt, M., Ploegh, H.L., and Lagaudrière-Gesbert, C. (2002). Analysis of protease activity in live antigen-presenting cells shows regulation of the phagosomal proteolytic contents during dendritic cell activation. J. Exp. Med. *196*, 529–540.

Mantegazza, A.R., Savina, A., Vermeulen, M., Pérez, L., Geffner, J., Hermine, O., Rosenzweig, S.D., Faure, F., and Amigorena, S. (2008). NADPH oxidase controls phagosomal pH and antigen cross-presentation in human dendritic cells. Blood *112*, 4712–4722.

Nair-Gupta, P., Baccarini, A., Tung, N., Seyffer, F., Florey, O., Huang, Y., Banerjee, M., Overholtzer, M., Roche, P.A., Tampé, R., et al. (2014). TLR signals induce phagosomal MHC-I delivery from the endosomal recycling compartment to allow cross-presentation. Cell *158*, 506–521.

Pierre, P., Turley, S.J., Gatti, E., Hull, M., Meltzer, J., Mirza, A., Inaba, K., Steinman, R.M., and Mellman, I. (1997). Developmental regulation of MHC class II transport in mouse dendritic cells. Nature *388*, 787–792.

Platt, C.D., Ma, J.K., Chalouni, C., Ebersold, M., Bou-Reslan, H., Carano, R.A.D., Mellman, I., and Delamarre, L. (2010). Mature dendritic cells use endocytic receptors to capture and present antigens. Proc. Natl. Acad. Sci. USA *107*, 4287–4292.

Reis e Sousa, C. (2006). Dendritic cells in a mature age. Nat. Rev. Immunol. *6*, 476–483.

Sallusto, F., and Lanzavecchia, A. (1994). Efficient presentation of soluble antigen by cultured human dendritic cells is maintained by granulocyte/macrophage colony-stimulating factor plus interleukin 4 and downregulated by tumor necrosis factor alpha. J. Exp. Med. *179*, 1109–1118.

Samie, M., and Cresswell, P. (2015). The transcription factor TFEB acts as a molecular switch that regulates exogenous antigen-presentation pathways. Nat. Immunol. *16*, 729–736.

Savina, A., and Amigorena, S. (2007). Phagocytosis and antigen presentation in dendritic cells. Immunol. Rev. *219*, 143–156.

Savina, A., Jancic, C., Hugues, S., Guermonprez, P., Vargas, P., Moura, I.C., Lennon-Duménil, A.-M., Seabra, M.C., Raposo, G., and Amigorena, S. (2006). NOX2 controls phagosomal pH to regulate antigen processing during crosspresentation by dendritic cells. Cell *126*, 205–218.

Savina, A., Peres, A., Cebrian, I., Carmo, N., Moita, C., Hacohen, N., Moita, L.F., and Amigorena, S. (2009). The small GTPase Rac2 controls phagosomal alkalinization and antigen crosspresentation selectively in CD8(+) dendritic cells. Immunity *30*, 544–555.

Savina, A., Vargas, P., Guermonprez, P., Lennon, A.-M., and Amigorena, S. (2010). Measuring pH, ROS production, maturation, and degradation in dendritic cell phagosomes using cytofluorometry-based assays. Methods Mol. Biol. *595*, 383–402.

Sepulveda, F.E., Maschalidi, S., Colisson, R., Heslop, L., Ghirelli, C., Sakka, E., Lennon-Duménil, A.M., Amigorena, S., Cabanie, L., and Manoury, B. (2009). Critical role for asparagine endopeptidase in endocytic Toll-like receptor signaling in dendritic cells. Immunity *31*, 737–748.

Spörri, R., and Reis e Sousa, C. (2005). Inflammatory mediators are insufficient for full dendritic cell activation and promote expansion of CD4+ T cell populations lacking helper function. Nat. Immunol. *6*, 163–170.

Stuart, L.M., and Ezekowitz, R.A. (2005). Phagocytosis: elegant complexity. Immunity *22*, 539–550.

Trombetta, E.S., Ebersold, M., Garrett, W., Pypaert, M., and Mellman, I. (2003). Activation of lysosomal function during dendritic cell maturation. Science *299*, 1400–1403.

Vega-Ramos, J., Roquilly, A., Zhan, Y., Young, L.J., Mintern, J.D., and Villadangos, J.A. (2014). Inflammation conditions mature dendritic cells to retain the capacity to present new antigens but with altered cytokine secretion function. J. Immunol. *193*, 3851–3859.

Wagner, C.S., and Cresswell, P. (2012). TLR and nucleotide-binding oligomerization domain-like receptor signals differentially regulate exogenous antigen presentation. J. Immunol. *188*, 686–693.

Wang, T., and Hong, W. (2002). Interorganellar regulation of lysosome positioning by the Golgi apparatus through Rab34 interaction with Rab-interacting lysosomal protein. Mol. Biol. Cell *13*, 4317–4332.

West, M.A., Wallin, R.P.A., Matthews, S.P., Svensson, H.G., Zaru, R., Ljunggren, H.-G., Prescott, A.R., and Watts, C. (2004). Enhanced dendritic cell antigen capture via toll-like receptor-induced actin remodeling. Science *305*, 1153–1157.

Wilson, N.S., Behrens, G.M., Lundie, R.J., Smith, C.M., Waithman, J., Young, L., Forehan, S.P., Mount, A., Steptoe, R.J., Shortman, K.D., et al. (2006). Systemic activation of dendritic cells by Toll-like receptor ligands or malaria infection impairs cross-presentation and antiviral immunity. Nat. Immunol. *7*, 165–172.

Zou, L., Zhou, J., Zhang, J., Li, J., Liu, N., Chai, L., Li, N., Liu, T., Li, L., Xie, Z., et al. (2009). The GTPase Rab3b/3c-positive recycling vesicles are involved in cross-presentation in dendritic cells. Proc. Natl. Acad. Sci. USA *106*, 15801–15806.